Desalination and Water Treatment
www.deswater.com

doi: 10.5004/dwt.2023.29780

303 (2023) 160–170
August

Integrated Fenton-like and photocatalytic system for metronidazole degradation in water using $FeNi_3/SiO_2/CuS$ magnetic nanocomposite

Negin Nasseh[a,b], Abolfazl Karimi Pour[c], Moslem Azqandi[d], Waleed M.S. Kassim[e], Behnam Barikbin[f,*], Tariq J Al-Musawi[g,*]

[a]*Cellular and Molecular Research Center, Birjand University of Medical Sciences, Birjand, Iran*
[b]*Department of Health Promotion and Education, School of Health, Birjand University of Medical Sciences, Birjand, Iran, Tel.: +985632381690; email: Negin.nasseh2020@gmail.com*
[c]*Department of Inspection Engineering, Abadan Faculty of Petroleum Engineering, Petroleum University of Technology, Abadan, 63187-14331, Iran, Tel.: +985632381690; email: AbolfazlKarimiPour1998@gmail.com*
[d]*Student Research Committee, Birjand University of Medical Sciences, Birjand, Iran, Tel.: +985632381690; email: Moslem.azq4@gmail.com*
[e]*Department of Petroleum and Gas Refinery Engineering, Al-Farabi University College, Baghdad, Iraq, email: Wesal.abedalrzaq@gmail.com*
[f]*Department of Environmental Health Engineering, School of Health, Social Determinants of Health Research Center, Mashhad University of Medical Sciences, Mashhad, Iran, Tel.: +985632381690; email: Barikbinb@mums.ac.ir*
[g]*Al-Mustaqbal University, Building, and Construction Techniques Engineering Department, Hillah 51001, Iraq, email: tariq.jwad@mustaqbal-college.edu.iq*

Received 28 January 2023; Accepted 28 June 2023

ABSTRACTS

In the present study, the adsorption mechanism and capacity of $FeNi_3/SiO_2/CuS$ magnetic nanocomposite, as a catalyst, for metronidazole (MTZ) antibiotic degradation were investigated. The degradation reaction was performed using an integrated treatment system comprised of Fenton-like and UV-photocatalytic processes. Various material analyses such as field-emission scanning electron microscope, Fourier-transform infrared spectroscopy, transmission electron microscopy, energy-dispersive X-ray analysis, X-ray diffraction, and vibrating-sample magnetometer were employed to prove the successful synthesis of the used catalyst and to gather information about its surface and structural properties. The characterization results showed that the nanocomposite used in this study was superparamagnetic (20 emu/g) and its crystal size was 26 and its particle size was about 64 nm. In addition, the effects of pH 3, 5, 7, 9, and 11, catalyst dosage $FeNi_3/SiO_2/CuS$ 0.005–0.1 g/L, initial metronidazole concentration 10–30 mg/L, contact time 5–200 min, and hydrogen peroxide content 50–200 mg/L, were studied. The $FeNi_3/SiO_2/CuS$ in the proposed treatment system was operated with MTZ degradation efficiency reach to 100% during the first 60 min of the degradation process. After the sixth cycle of regeneration processes, the $FeNi_3/SiO_2/CuS$ lost only 5% of its degradation ability (from 100% to 96.83%). The degradation efficiency of the chemical oxygen demand (COD) parameter was tested which is remarkably enhanced to ~74% during degradation time of 200 min. Also, the analysis of COD on real wastewater at this time showed a reduction of about 65.8% during this process under optimal reaction conditions. The adsorption followed a pseudo-first-order kinetic equation ($R^2 \geq 0.9$). Taking the results of this study, the $FeNi_3/SiO_2/CuS$ shows a potential application as a catalyst for MTZ degradation using photocatalytic combined with a Fenton-like treatment system.

Keywords: Metronidazole; Degradation; $FeNi_3/SiO_2/CuS$; Characterization; Kinetic

* Corresponding authors.

1. Introduction

Pharmaceutical compounds, in the environment, are a group of organic contaminants that can seriously damage the quality of water bodies and causes a variety of adverse effects on the environment and humans alike [1]. Antibiotics are among the most prevalent pharmaceutical pollutants in the environment due to their widespread use in hospitals and agricultural fields [2]. Metronidazole (MTZ) is one of the examples of effective antibiotics that are used to treat parasitic and bacterial infections that affect humans and animals and for this reason, it has gained wide fame in the pharmaceutical industry. To control and not spread this pollutant in the environment, environmental organizations have set a maximum concentration of MTZ in the wastewater so that its concentration does not exceed 0.1 mg/L [3].

Advanced oxidation processes (AOPs) are one of the most effective methods currently used in the treatment of organic or non-biodegradable pollutants, including antibiotics [4]. These processes produce high-reactive radical species (like hydroxyl radical (•OH)), which can significantly oxidize various toxic pollutants [5,6]. In addition, in AOPs comprise using strong reactive oxidant species such as ozone (O_3), hydrogen peroxide (H_2O_2), and catalyst (e.g., iron, transition metals, semi-conductor solids). The used catalyst in AOPs can be activated in the presence of an energy source like lights (UV, visible, and sun lights) or ultrasonic waves [6]. In fact, •OH radical has non-selectivity performance and consider the main oxidative parameter in AOPs with the potential oxidation of 2 and 2.8 eV for pH values of zero and 14, respectively [7].

Fenton and Fenton-like reagents. They are formed based on the iron ions (Fe^{2+}, Fe^{3+}) and hydrogen peroxide (H_2O_2), which are utilized as one of the most efficient strategies of AOPs for the degradation and mineralization of non-biodegradable contaminants [5]. Simple technology, relatively low-cost, high •OH productivity, running in ambient temperature, reagent accessibility, and ease of maintenance and storage are the unique advantages of this method [7,8]. However, due to complications like (A) short-range of pH 2–4, (B) the production of sludge that contains iron ions, which is not possible to recover them after the oxidative process, and (C) the requirement of a large concentration of iron ions 50–80 mg/L is higher than 2 mg/L, making this process economically inefficient to use, according to the standards of purified water in the European Union [8,9].

Recently, Fenton and heterogeneous Fenton-like processes have been studied to address homogeneous Fenton processes' drawbacks [10–12]. Most catalysts that were applied in the heterogeneous Fenton-like processes have porous structures with sizes in the scale of nano and micro. Therefore, in some cases, they have higher pollutants adsorption on their surface than homogeneous Fenton processes in removal performance [13]. Other advantages which can be mentioned are related to heterogeneous Fenton-like processes such as a broad range of pH, ease of recovery of nanoparticles, simple synthesis, and exemplary performance in destroying organic materials [9]. In some studies, to increase the catalytic process, an external energy source is also considered, like ultrasonic, electricity, and Futons assisted with the catalyst [5,7]. Based on it, various studies for removing organic substances from aqueous solutions utilizing heterogeneous Fenton-like catalyst processes have been carried out [14–16].

Magnetic $FeNi_3$ alloy is a nanoparticle-based on iron, which has superior properties, such as high magnetics, high permeability, low energy loss, and high temperature. These features make it suitable to be used as a catalyst in heterogeneous Fenton-like processes for destroying different organic materials from aquatic environments [17]. The existence of iron and nickel on $FeNi_3$ chemically makes it high-active. As a result of the exposure to air, they can show reactions and become oxidized. According to it, the stability of $FeNi_3$ for a long time without accumulation and precipitation is of great importance [18].

Consequently, developing nanocomposite with a protective strategy prevents the instability of nanoparticles as core-shell structures [19]. For this purpose, the shell structure avoids reaching oxygen to the core surface [18]. The aim of nanocomposite synthesis can be varied, including (A) high degradation efficiency, (B) increasing light absorption, (C) enhancement of efficient separation, and (D) access to stability and reusability [20,21]. This strategy involves covering nanoparticles with organic matter like polymers or minerals like silica (SiO_2) and carbon [18,19]. In addition, covered nanoparticles with SiO_2 can accelerate the decompositions of H_2O_2 to •OH, increasing the rate of degradation of organic contaminants [22]. Moreover, SiO_2 can increase the adsorption of contaminants on nanoparticles that are used as catalysts [23].

Since heterogeneous reactions are dependent on Fe^{3+} (oxidant agent) and also the catalytic speed of the heterogeneous reaction is much slower than the homogeneous reaction [Eqs. (1) and (2)], increasing Fe^{2+} generation will be crucial. Accordingly, using the semiconductor accompanied by heterogeneous catalysts can increase the activity of heterogeneous Fenton-like processes due to the presence of photoelectrons. The presence of photoelectrons in the reaction can cause the reduction of Fe^{3+} to Fe^{2+} [Eqs. (3) and (4)]. On the other hand, the ultraviolet (UV) light simultaneously increases the regeneration of Fe^{2+} and the production of •OH [Eqs. (5) and (6)] [24].

$$Fe^{2+} + H_2O_2 \rightarrow Fe^{3+} + OH^- + {}^{\bullet}OH \quad \left(k_1 = 76\ 1/M.s\right) \tag{1}$$

$$Fe^{3+} + H_2O_2 \rightarrow Fe^{2+} + {}^{"}OH \quad \left(k_2 = 0.001 \circledcirc 0.01\ 1/M.s\right) \tag{2}$$

$$\text{Semi} - \text{conductor} + h½ \rightarrow e^- + h^+ \tag{3}$$

$$Fe^{3+} + e^- \rightarrow Fe^{2+} \tag{4}$$

$$Fe\left(OH\right)^{2+} + h½ \rightarrow Fe^{2+} + {}^{\bullet}OH \tag{5}$$

$$H_2O_2 + h½ \rightarrow 2\,{}^{\bullet}OH \tag{6}$$

Copper sulfide (CuS) is a semiconductor (a bandgap of 2 eV) that has attracted so much attention for removing organic compounds from aquatic environments because of its high photocatalytic potential in the presence of UV irradiation. The main advantages of this substance are the ability

to adsorb a wide variety of electromagnetic waves and high efficiency in the photocatalytic degradation of organic compounds. Furthermore, non-toxicity, no limitation of mass transfer, performance in environmental conditions, high chemical stability in a broad range of pH, high resistance against chemical decomposition, and light corrosion can be mentioned as crucial advantages of this catalyst [18].

Therefore, to overcome the drawbacks of separating using traditional Fenton and photocatalytic methods in the degradation of pollutants, and on the other hand, the very good capability of the composite $FeNi_3/SiO_2/CuS$ in removing antibiotics during the photocatalyst process, this study aims to investigate the degradation of metronidazole from aqueous environments using heterogeneous Fenton-like photocatalytic integrated process.

2. Materials and method

2.1. Chemicals

MTZ powder, whose chemical properties are mentioned in Table 1, with a purity percentage of ≥95%, was purchased from Sigma-Aldrich Company (Munich, Germany). Preparation and dilution of the stock solution of MTZ (1,000 mg/L) and other used solutions were carried out using deionized water during all experiments. To avoid instability and keep MTZ safe, the solution was maintained in dark conditions at 4°C for a week. In addition, polyethylene glycol-600 (PEG-6000,1.0 g MW), nickel chloride ($NiCl_2{\cdot}6H_2O$), hydrazine hydrate ($N_2H_4{\cdot}H_2O$, purity percentage 80%), tetraethyl orthosilicate ($SiC_8H_{20}O_4$, TEOS), ammonia (NH_3), copper sulfate ($CuSO_4$), ethylene glycol ($C_2H_6O_2$), and sodium thiophosphate ($Na_2S_2O_3$) were provided form Merck Company (Germany) for the synthesis of the nanocomposite ($FeNi_3/SiO_2/CuS$). Hydrogen peroxide was also purchased for the heterogeneous Fenton-like experiments from this company.

2.2. Materials

In this experimental study, for providing a light source, a UV lamp (TUV PHILIPS PL-L) with 18 W, wavelength of 254 nm, and radiation intensity of 2,500 mc·W/cm^2 was utilized. This light bulb was located in a quartz sheath in the center of the designed reactor (made of steel). The temperature of the reactor was regulated in the range of 24°C ± 2°C. A wall of cooling water was used around the quartz sheath. Samples were collected after determined time intervals and were analyzed. The reactor used in this research is shown in Fig. 1.

2.3. $FeNi_3/SiO_2/CuS$ synthesis

The synthesis process of magnetic nanocomposite $FeNi_3/SiO_2/CuS$ was carried out in two steps based on the following methodology: first, $FeNi_3/SiO_2$ nanoparticle was synthesized according to past studies [25]. Secondly, to cover a $FeNi_3/SiO_2$ by CuS, 0.15 g of it was added to 20 mg of ethylene glycol and then dispersed for 30 min in an ultrasonic device. Afterward, the dispersed materials were poured into a 500 cc balloon and then kept in an oil bath at 120°C. Subsequently, 0.8 g of copper sulfide ($CuSO_4$) was added to the mentioned suspension, and the balloon's contents were completely dissolved. The resulting suspension is shown by A notation. Following this, 1.9 g of sodium thiosulfate ($Na_2S_2O_3$) was separately added to 20 mg of ethylene glycol, which was named suspension B. Next, suspension B was added to the suspension containing $FeNi_3/SiO_2$ (A), and the final sample was operated at 140°C for 90 min to reflux. Finally, following a certain time and cooling down the balloon, the prepared products were washed with ethanol once, deionized water several times, and separated using an N_{42} magnet. In the end, it dried in the oven (80°C) for 5 h [26].

2.4. Characterization analysis

$FeNi_3/SiO_2/CuS$ magnetic nanocomposite was characterized using different devices; for analyzing surface

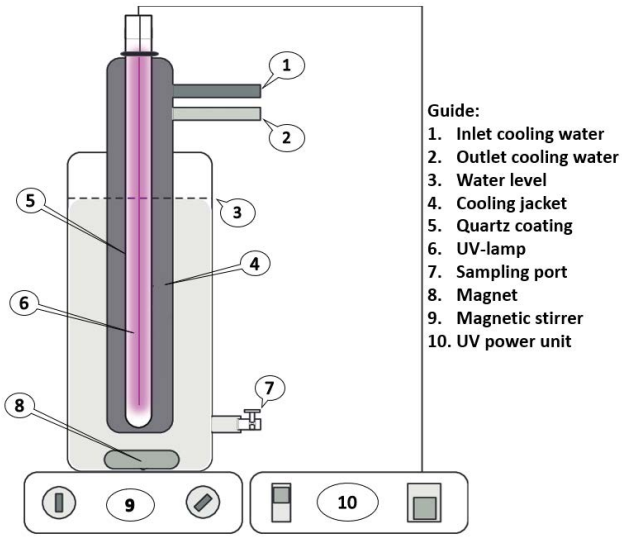

Fig. 1. Schematic diagram of the used reactor.

Table 1
Pseudo-first-order kinetic model for MTZ degradation by $FeNi_3/SiO_2/CuS/UV/H_2O_2$ process, where $t_{1/2} = 0.693/K_0$

Concentration (mg/L)	Equation	K_0 (1/min)	R^2	$t_{1/2}$ (min)
10	$Y = 0.1343x + 1.1795$	133.4×10^{-3}	0.9807	5.19
15	$Y = 0.062x + 1.372$	62×10^{-3}	0.9786	11.18
20	$Y = 0.0378x + 1.5271$	37.8×10^{-3}	0.9879	18.33
25	$Y = 0.0152x + 1.5452$	15.2×10^{-3}	0.9264	45.59
30	$Y = 0.0089x + 1.4121$	8.9×10^{-3}	0.9398	77.86

morphology (the study of form, mean diameter, and details of the synthesized nanocomposite surface), a field-emission scanning electron microscope (FE-SEM); (Germany, Zeiss Sigma VP-500) and also a transmission electron microscopy (TEM) (Germany, Zeiss-EM10C-100 KV) were used to investigate the topographical and morphological properties of the synthesized materials. Additionally, for detecting the presence of elements in the magnetic nanocomposite, energy-dispersive X-ray analysis (EDX) was used. Analyzing the functional groups of the magnetic nanocomposite was done using Fourier-transform infrared spectroscopy (FTIR). The magnetic property of the nanocomposite was carried out by the vibrating-sample magnetometer (VSM) device (VSM 7400). Eventually, the crystal structure of $FeNi_3/SiO_2/CuS$ was observed using X-ray diffraction (XRD; X'Pert PRO made by PANalytical Company).

2.5. MTZ degradation experiments

In the current study, all of the MTZ degradation experiments were carried out in a nonstable equilibrium system under the following condition: In all experiments, the solution volume was 400mL. A magnetic stripper was used to mix the samples at 350 rpm. Hydrochloric acid (HCl) and sodium hydroxide (NaOH) were used to adjust pH. The operating parameters in the study of MTZ degradation were pH 3, 5, 7, 9, and 11, the dosage of magnetic nanocomposites 0.005, 0.01, 0.02, 0.03, 0.04, 0.05 and 0.1 g/L, initial concentration of MTZ 10, 15, 20, 25 and 30 mg/L, contact time 5, 10, 15, 30, 60, 90, 180 and 200 min, and hydrogen peroxide concentration 50, 100, 150 and 200 mg/L. The residual amount of MTZ was analyzed using spectrophotometer (T80$^+$ UV/Visible) at a wavelength of 320 nm [27]. To minimize the interference effect of H_2O_2 in experimental findings, 200 μL of $Na_2S_2O_3$ (0.2 N) was added to samples containing hydrogen peroxide were added, and then the concentration of contaminants was measured [28]. In addition, to investigate the accuracy of experimental results, each experiment was repeated three times and their average value was reported.

To calculate the efficiency of the MTZ degradation process, Eq. (7) was used in which MTZ_0 and MTZ_t are the initial and final concentrations of metronidazole, respectively (mg/L). R (%) is equal to the percentage of metronidazole elimination [29].

$$R(\%) = \left[\frac{(MTZ_0 - MTZ_t)}{MTZ_0}\right] \times 100 \tag{7}$$

Furthermore, the degradation rate of the suggested treatment process is generally described by the pseudo-first-order kinetic model, which can be explained under the model of Langmuir–Hinshelwood (L–H) [30]:

$$-\frac{dC}{dt} = k_{obs}C \tag{8}$$

$$\ln\left(\frac{C}{C_0}\right) = -k_{obs}t \tag{9}$$

where k_{obs} is the rate constant of pseudo-first-order (1/min), t is the time reaction (min), C is the residual concentration after the oxidation time and C_0 is the initial concentration of contaminant (mg/L).

Since one of the foremost effective methods to assess the effect of the photocatalytic process for removing wastewater containing organic substances such as in pharmaceutical factories is chemical oxygen demand (COD) determination [31]. In this study, the actual wastewater was manually collected from one of the well-known drug production companies in Iran, Tehran. Firstly, the amount of COD was measured (Lovibond COD VARIO Checkit Direct/Germany) in the natural wastewater, which constituted 701 mg/L. Next, the sample was placed in the reactor without considering pH adjustment accompanied by a specific concentration of the nanocomposite in the presence of UV irradiation and hydrogen peroxide in the determined interval times 5, 10, 15, 30, 60, 90, 180 and 200 min. The samples were taken from the reactor, and their COD values were measured. Also, in real wastewater, various salts, anions, and cations are found, which can have interference effects on the treatment process. Thereafter, a particular concentration (20 mg/L) of MTZ was added to real wastewater and was measured by the spectrophotometer device. Following this, according to optimal conditions obtained from synthetic wastewater, it was placed in the reactor and at different times, metronidazole concentration was measured in the natural wastewater.

2.6. Regeneration test

One of the important parameters to evaluate the activity and stability of solid catalysts is recycling them. Hence, in this work, to investigate the reusability of the synthesized nanocomposite, metronidazole degradation experiments were carried out in six periodic cycles under optimal conditions (metronidazole's concentration 20 mg/L, catalyst dose 0.01 g/L, contact time 200 min, hydrogen peroxide's concentration 150 mg/L and pH = 7). The nanocomposite was separated from the solution by a magnet after each cycle and then washed several times using deionized water in an oven at 80°C. In the end, the residual concentration of MTZ was measured after each cycle.

2.7. COD and total organic carbon analysis

To assess the mineralization decay of MTZ degradation, the total organic carbon (TOC) analyzer (ANA TOC, made in SGE Co., Australia) and the COD analyzer (Lovibond COD Vario Checkit Direct, Germany) were employed to determine the TOC and COD concentrations, respectively. These analyses were conducted based on the standard method and were examined under optimized operating conditions.

3. Results and discussion

3.1. Characterization of the synthesized nanocomposite

In this study, the $FeNi_3/SiO_2/CuS$ synthesized magnetic nanocomposite was characterized using XRD, FTIR, FE-SEM, TEM, EDX, and VSM. The findings are shown in previse published articles [18].

According to the XRD pattern of $FeNi_3/SiO_2/CuS$ nanocomposite, the different peaks at 2θ values of 31.92, 32.98, 35.37, 43.08, 48.08, 52.77, and 59.41. these peaks are related to copper sulfide, which is in good agreement with those of copper sulfide obtained from the Joint Committee on Powder Diffraction Standards (JCPDS 01-079-2321). In addition, a wide peak in the range of 2θ from 10 to 20 is observed, which is associated with the SiO_2 layer. There are three peaks in the range of 44.22, 53.56, and 75.47, which correspond to the magnetic core of $FeNi_3$ (ICSD Collection Cod: 040,334). It is worth mentioning that the size of synthesized nanocomposites was calculated by Debye–Sherrer's Equation [Eq. (10)]. Based on the full width at half maximum, the highest peak of diffraction was determined to be 26 nm.

$$D = \frac{0.98\lambda}{\beta\cos\theta} \tag{10}$$

where D = particle diameter, β = peak width half-height, θ = diffraction angle at peak, λ = X-ray wavelength (λ = 0.154 nm).

Based on FTIR analysis of $FeNi_3/SiO_2/CuS$ magnetic nanocomposite, the peak at 490.84 1/Cm is assigned to the vibration of metal bands with a sulfur heteroatom, which the most probable bond is Cu–S. The relatively strong bond at 637.00 1/Cm is due to the vibration of various metal bands like Fe–Ni–Fe–Ni or Fe–Ni–Ni. The weak absorption bond is observed at 918/96 1/Cm, corresponding to Ni–Cu, Fe–Cu, or Fe–Ni–Cu vibrations. Two reinforced bands are seen at 1,140.06 and 1,015.79 1/Cm, which can be due to the presence of the vibration of the bond between Si–O, Fe–SiO_2, or Ni–Fe–SiO_2. Eventually, the bands in the absorption spectrum detected at 1,397.05 and 1,511.46 1/Cm are attributed to the vibration of bonds between C–O, C–N, or C–H, stemming from the impurity of initial materials such as polyethylene glycol or hydrazine hydrate. Also, the FE-SEM depicts the surface morphology of the synthesized nanocomposites as core-shell-shell. According to the obtained micrograph from synthesized nanocomposite, the size of the nanoparticles is in the range of 26–64 nm, indicating that the material has magnetic properties and has the tendency to accumulate. The agglomeration feature can be due to the magnetic characteristic of the nanocomposite, whether the different particles or parts of the material absorbed each other or were located alongside each other.

TEM image was also obtained with the magnification of 46460 KX, demonstrating that the synthesized nanocomposites are amorphous and cannot be suggested as regular structures. Given the agglomeration of material texture, the density of the synthesized nanocomposite is high. Furthermore, based on the nanocomposite's EDX of this nanocomposite, all elements of the nanocomposite exist in the test result, which proves the accuracy of the synthesis. In the sample, the highest and lowest concentration of the elements is allocated to Cu and Si, respectively.

The synthesized nanocomposite was evaluated using VSM magnetic analysis at room temperature to analyze the magnetic properties. The magnetic moment vs. magnetic field (M-H loop) at 300 K for $FeNi_3/SiO_2/CuS$ has been shown in previous papers and has been avoided from repeating the image. The obtained magnetic curves show the magnetic saturation of the nanocomposite is 20 emu/g. Consequently, it can be concluded that the nanocomposite is dispersed in water and can be collected by an external magnetic field quickly and then easily spread with a slight twitch.

3.2. Effect of pH

In this part of the research, the results of solutions' pH and contact time effects in the oxidative process of MTZ in the presence of UV and H_2O_2 using synthesized magnetic nanocomposite are presented.

As can be seen in Fig. 2, the highest and lowest percentage of metronidazole removal using $FeNi_3/SiO_2/CuS/H_2O_2$ was obtained at pH of 7 and 11, respectively.

According to previous studies, pH changes have no significant effect on metronidazole elimination in aquatic environments using AOPs such as photocatalysts. In other words, pH is not the determining factor in AOPs. Pan et al. [32] removed metronidazole in Fenton-like process. The results obtained from this research also confirm the results obtained from this study.

3.3. Effect of catalyst dose

The impact of $FeNi_3/SiO_2/CuS$ nanocatalyst dose and contact time was investigated in the presence of UV H_2O_2 for photocatalytic decomposition of metronidazole.

Fig. 3 demonstrates that the percentage of MTZ removal increased from 0.005 mg/L to 0.01 g/L by $FeNi_3/SiO_2/CuS/UV/H_2O_2$ process. Conversely, the impact of higher doses of the aforementioned nanocomposite on MTZ removal showed a noticeable decrease. That is to say, the removal efficiency of MTZ rose from 85.89% to 91.16% by adding catalyst concentration 0.005–0.01 g/L and then declined remarkably to 56% with an increase higher catalyst dose than 0.01 g/L during 60 min.

The changes can be attributed to more absorbed photons with the increase of nanocomposite concentration, which leads to the rise of activated sites and enhances the number of absorbed metronidazole molecules [33]. The main reason for the reduction in removal efficiency of MTZ by heterogeneous Fenton-like process is the excessive elevating

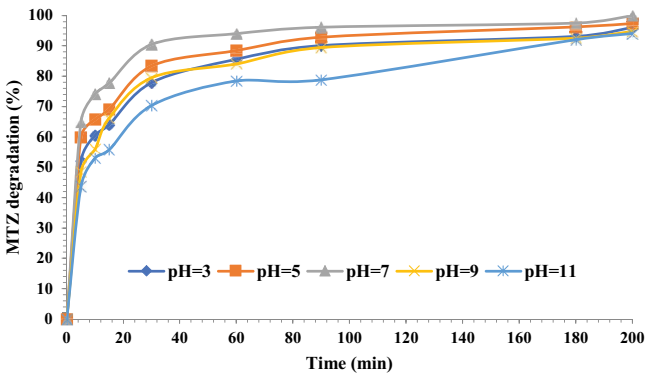

Fig. 2. Effect of various pH on the concentration of metronidazole elimination in the $FeNi_3/SiO_2/CuS/UV/H_2O_2$ process (concentration of MTZ: 20 mg/L, catalyst dosage: 0.02 g/L, concentration of hydrogen peroxide: 150 mg/L, ambient temperature).

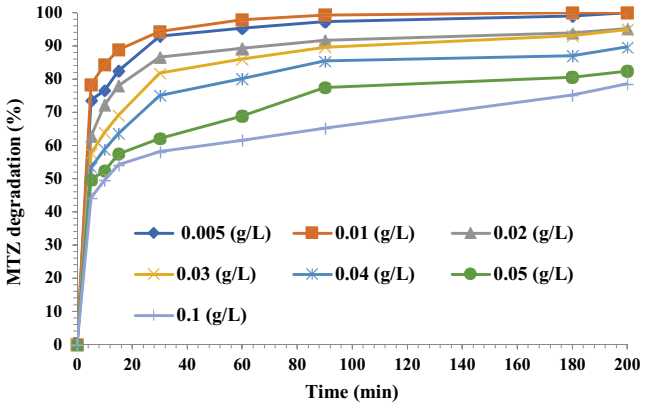

Fig. 3. Effect of various magnetic nanocomposite concentrations on metronidazole removal efficiency in $FeNi_3/SiO_2/CuS/UV/H_2O_2$ process (pH = 7, contaminant concentration: 20 mg/L, hydrogen peroxide concentration: 150 mg/L, ambient temperature).

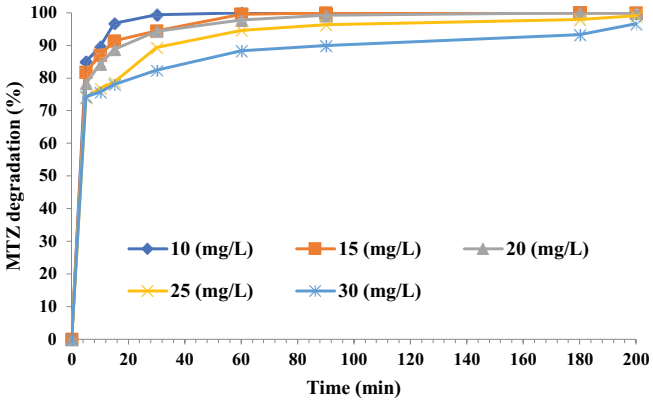

Fig. 4. Effect of various initial concentration of metronidazole on the $FeNi_3/SiO_2/CuS/UV/H_2O_2$ process (pH = 7, catalyst concentration: 0.01 g/L, hydrogen peroxide: 150 mg/L, ambient temperature).

of catalyst concentration, which can cause significant problems for the treatment system such as turbidity, light dispersion, and accumulation and precipitation of nanocomposite [34,35]. As mentioned, increasing the catalyst concentration decreases the elimination efficiency of metronidazole. It demonstrates that the lower nanocomposite dose has desirable pollutant degradation efficiency. Overall, advanced oxidation processes based on photocatalysts have a rapid rate of contaminant degradation by enhancing catalyst concentration. On the other hand, high concentrations of nanocatalysts have adverse effects on the rate of photocatalytic reaction, causing the reduction of UV light absorption to the surface of the catalyst [34].

In a study, the efficiency of metronidazole removal by the photocatalytic process based on zinc oxide nanoparticles was performed. The findings revealed that the MTZ removal rate increased substantially with rising catalyst content from 0.5 to 1.5 g/L, which declined with elevating catalyst concentration to 3 g/L [36]. Ni et al. [37] evaluated the ability of $g\text{-}C_3N_4/TiO_2$ photocatalyst to degrade TC under UV radiation. The results showed that the degradation rate of TC increased when the photocatalytic amount of $g\text{-}C_3N_4/TiO_2$ increased from 0.6 g/L to 1 g/L. On the contrary, the photocatalytic amount was decreased with the additional dose of nanocomposite up to 1.2 g/L.

3.4. Effect of MTZ concentration

The results of the simultaneous effects of metronidazole's initial concentration 10, 15, 20, 25, and 35 mg/L and contact time 5–200 min on the photocatalytic process in the presence of UV and H_2O_2 are presented in the following graph, at the optimization value of pH and nanocomposite concentration.

As shown in Fig. 4, increasing the initial concentration of MTZ causes a remarkable decline in its removal efficiency using $FeNi_3/SiO_2/CuS/UV/H_2O_2$ process.

The decrease in the amount of removal due to the increase in the concentration of the studied antibiotics can be explained as follows: considering that the amount of $FeNi_3/SiO_2/CuS$ nanocomposite is the same in all concentrations, as well as the pH value, the radiation intensity of each of light (ultraviolet), contact time and concentration of hydrogen peroxide are also the same, as a result, the radicals produced are also the same in all 5 concentrations. Therefore, metronidazole removal will be more in samples with lower concentrations. The second reason for this phenomenon is that elevating pollutant content leads to inaccessible UV irradiation to be absorbed on the surface of the nanocomposite [38,39].

The ultimate reason is associated with absorption between the vast number of pollutant molecules and surface catalysts as a result of the rise of initial contaminant concentration. Therefore, it prevents the reaction between the produced photon holes and hydroxyl radicals. Azimi and Nezamzadeh-Ejhieh [39] reported the degradation of tetracycline and cephalexin by clinoptilolite coated with PbS-CdS as a photocatalytic process from aquatic environments. Zhou et al. [40] attempted to eliminate Tetracycline using microporous nanocomposite Cu_2O/ZIF-8 in the presence of visible light. The results demonstrated a significant fall in the removal efficiency of pollutants by increasing the initial concentration of tetracycline from 10 to 50 mg/L.

3.5. Effect of H_2O_2 concentration

The simultaneous effect of H_2O_2 50, 100, 150, and 200 and contact time 5–200 min in metronidazole degradation utilizing $FeNi_3/SiO_2/CuS/UV/H_2O_2$ process are presented in the section.

Fig. 5 demonstrates the positive effect of elevated amounts of hydrogen peroxide on metronidazole elimination efficiency by $FeNi_3/SiO_2/CuS/UV/H_2O_2$. The concentration of H_2O_2 is a significant factor in the decontamination of organic matter in Fenton-like processes [41]. Since the number of produced hydroxyl radicals is related to the efficiency of the degradation process, increasing the concentration of hydrogen peroxide remarkably destroys MTZ molecules. Several studies have proven that adding hydrogen peroxide content can boost the degradation process-based photocatalyst.

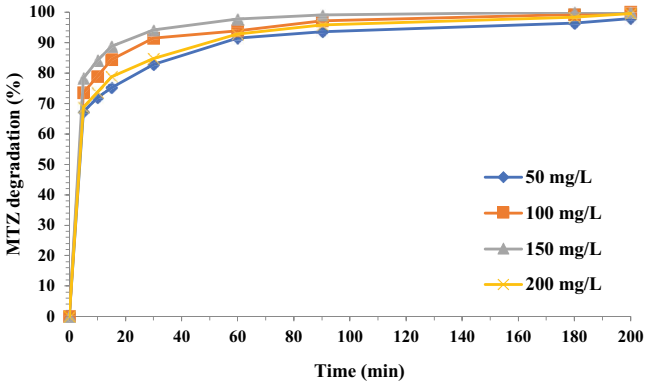

Fig. 5. Effect of various hydrogen peroxide concentrations on the elimination of metronidazole using $FeNi_3/SiO_2/CuS/UV/H_2O_2$ process (pH = 7, contaminant concentration: 20 mg/L, catalyst dose: 0.01 g/L, ambient temperature).

Consequently, choosing a suitable amount of hydrogen peroxide proportional to pollutant concentration is more important. It seems that this oxidant agent has two roles in the process of photocatalytic oxidation. According to the following equations, hydroxyl radical species are mainly generated [42]:

$$H_2O_2 + e^- \rightarrow OH^- + OH^\bullet \quad (11)$$

$$H_2O_2 + O_2^{\bullet -} \rightarrow OH^\bullet + OH^- + O_2 \quad (12)$$

In addition, in heterogeneous photocatalytic Fenton-like processes, higher values of hydroxyl radical species are produced due to the decomposition of hydrogen peroxide.

As can be seen in Fig. 5, rising the concentration of hydrogen peroxide from 50 to 200 mg/L, the elimination percentage of metronidazole utilizing $FeNi_3/SiO_2/CuS/UV/H_2O_2$ firstly increased by adding hydrogen peroxide concentration from 50 to 150 mg/L, after which it decreased by further adding hydrogen peroxide content. This can be due to the excessive reaction between H_2O_2 and $OH^\bullet$, causing the formation of $HO_2^\bullet$ according to the following equations [43,44]:

$$OH^\bullet + H_2O_2 \rightarrow H_2O + HO_2^\bullet \quad (13)$$

$$H_2O_2 + h^+ \rightarrow H^+ + HO_2^\bullet \quad (14)$$

Cai et al. investigated the percentage of metronidazole elimination using the photo-Fenton process with a magnetic Fe_3O_4@PBC composite. The results showed that by increasing the concentration of hydrogen peroxide, the elimination efficiency of MTZ decreased, which is consistent with the results of this research [45].

3.6. Kinetic study

Fig. 6 and Table 1 show the kinetic for the removal of metronidazole antibiotic by the mentioned process.

Evaluating the kinetic degradation of organic pollutants using AOPs has demonstrated that the pseudo-first-order kinetic model is a fitted model to describe kinetic behaviors.

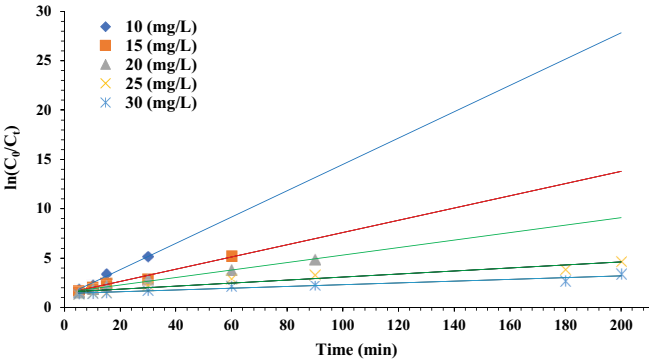

Fig. 6. Kinetic modeling of the MTZ experimental data and the pseudo-first-order kinetic model at different concentrations.

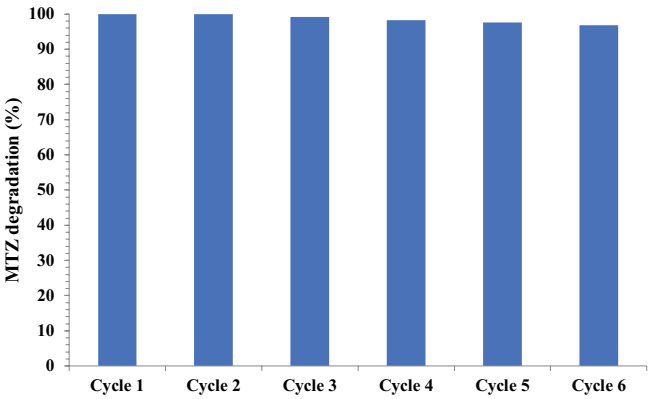

Fig. 7. Diagram of MTZ antibiotic degradation in $FeNi_3/SiO_2/CuS/UV/H_2O_2$ photocatalytic process in during 6 cycles of reuse.

In this work, the aforementioned model was used for analyzing the metronidazole's degradation kinetic; the results are shown in Fig. 6 and Table 1. As shown, an increase in the concentration of contaminants causes a drastic decline in the constant rate (k_{obs}). Farzadkia et al. [46] and Seidmohammadi et al. [47] also studied the kinetic evaluation of metronidazole elimination. Their results showed that the pseudo-first-order model is well-described in the kinetic trends of MTZ removal that correspond with the current study.

3.7. Regeneration study

According to Fig. 7, the experimental results indicated that the synthesized nanocomposite had a minor loss efficiency within 3.17% after the 6th run. This reduction efficiency can be ascribed to the mass reduction of synthesized nanocomposite during the recycling process. As a result, it can be understood that this synthesized nanocomposite has not been inactive and its applicability is cost-effective during heterogeneous photocatalytic Fenton-like processes.

3.8. Result of COD and TOC

Fig. 8. shows the removal rate of MTZ, TOC, and COD by $FeNi_3/SiO_2/CuS$ during 200 min of degradation time. It can be seen that approximately 100%, 65%, and 83.06% of

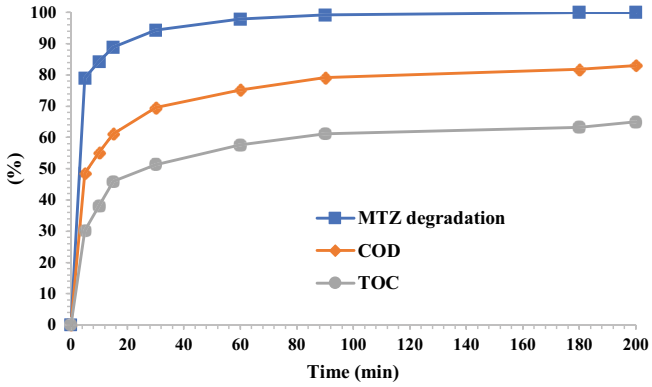

Fig. 8. Comparison of metronidazole removal percentage and chemical oxygen demand and total organic carbon reduction percentage.

MTZ removal efficiency, TOC, and COD removal efficiencies were achieved at 200 min of degradation time, respectively. Compared to the removal efficiency of MTZ, the mineralization degree is incomplete, which is attributed to the refractory of intermediate compounds generated during the MTZ photocatalytic reactions.

3.9. Mineralization study

COD and metronidazole concentration removal on real wastewater utilizing $FeNi_3/SiO_2/CuS/UV/H_2O_2$ process is represented in Figs. 9 and 10, respectively.

The results showed that hydrogen peroxide considered a strong and environmentally friendly oxidant, plays a crucial role in COD reduction in the photocatalytic processes. Under optimal conditions, the efficiency of COD removal by $FeNi_3/SiO_2/CuS/UV/H_2O_2$ was determined to be 65.8% within 200 min. In contrast, the percentage of COD reduction was recorded between 95% and 100% from synthetic wastewater containing MTZ by the above-mentioned photocatalytic process. Also, the residual concentration of MTZ reached 6.84 mg/L after a 200 min period of oxidation, where the constant content of MTZ was 20 mg/L. In the same operating conditions, the removal efficiency of MTZ stood at 74.48% in real wastewater. However, this efficiency was obtained within 180 min in the synthetic wastewater.

The main reason for the decrease in MTZ efficiency is high turbidity and various anions and antibiotics in different concentrations in synthetic wastewater.

The mentioned causes lead to a decline in light penetration, which can reduce the efficiency of CID removal throughout photocatalytic processes. According to these findings, $FeNi_3/SiO_2/CuS/UV/H_2O_2$ photocatalytic process is well-suited and cost-effective for COD elimination from various real wastewater. In the end, the present study revealed that organic carbon converts to mineral carbon in natural wastewater.

3.10. MTZ removal using different processes

Fig. 11 shows the removal efficiency of metronidazole by heterogeneous photocatalytic Fenton-like process ($FeNi_3/SiO_2/CuS/UV/H_2O_2$), photocatalytic process ($FeNi_3/$

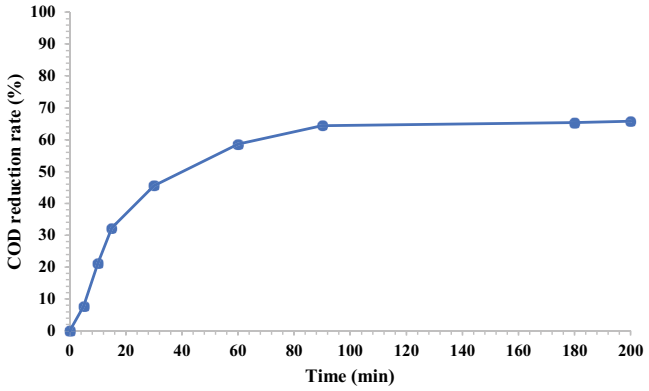

Fig. 9. Shows chemical oxygen demand removal of real wastewater by $FeNi_3/SiO_2/CuS/UV/H_2O_2$ process (pH = 7, nanocomposite dose: 0.01 g/L, hydrogen peroxide concentration: 150 mg/L and ambient temperature).

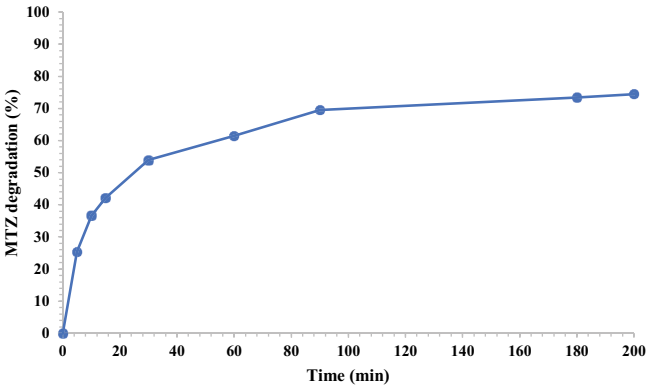

Fig. 10. Effect of different metronidazole concentrations in natural wastewater in the presence of UV and H_2O_2 (pH = 7, nanocomposite dose: 0.01 g/L, hydrogen peroxide concentration: 150 mg/L, contaminant concentration: 20 mg/L, and ambient temperature).

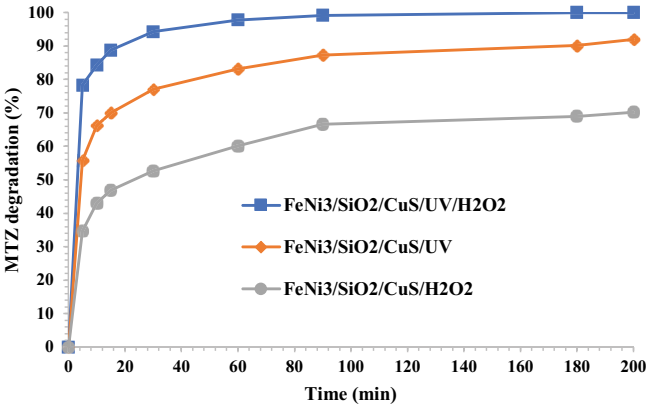

Fig. 11. Comparison of $FeNi_3/SiO_2/CuS/UV/H_2O_2$, $FeNi_3/SiO_2/CuS/UV$, and $FeNi_3/SiO_2/CuS/H_2O_2$ processes for MTZ degradation (pH = 7, nanocomposite dose: 0.01 g/L, hydrogen peroxide concentration: 150 mg/L, contaminant concentration: 20 mg/L and ambient temperature).

Table 2
Comparison of metronidazole removal from aqueous solutions in different processes using composite $FeNi_3/SiO_2/CuS$

No	Process	Metronidazole concentration (mg/L)	Equilibrium time (min)	Efficiency (%)
1	Adsorption	20	120	60.35
2	Heterogeneous Fenton-like	20	90	83.64
3	Photocatalyst	20	60	90.63
4	Heterogeneous Fenton-like photocatalytic	20	30	94.3

SiO_2/CuS/UV), and heterogeneous Fenton-like process ($FeNi_3/SiO_2/CuS/H_2O_2$).

Fig. 11 shows the photocatalytic performance of $FeNi_3/SiO_2$/CuS with the other photocatalytic-based processes. The results indicated that the photocatalytic process in the presence of UV light and H_2O_2 had superior efficiency compared to the other studied methods for MTZ degradation. This is mainly attributed to the participation of h^+ of the CuS conductive layer and a vast number of oxidant radical species in the semiconductor layer capacitance. Moreover, the $FeNi_3/SiO_2/CuS/UV/H_2O_2$ heterogeneous photocatalytic Fenton-like process not only has positive holes and radical species but also includes more produced radicals in the heterogeneous Fenton-like process, accelerating the process performance.

3.11. Compare with literature

As can be seen in Table 2, with the constancy of the composite as well as the concentration of metronidazole, the removal efficiency of this pollutant in different processes was compared with each other, and as can be seen in this table, the combined heterogeneous Fenton-like photocatalytic process in the least time is the most It has efficiency compared to three absorption processes, pseudo-Fenton heterogeneous and photocatalyst. This comparison shows the superiority of this process over other processes.

4. Conclusion

The studied results revealed that the heterogeneous photocatalytic Fenton-like process had a better degradation performance on MTZ removal than the sole process (heterogeneous Fenton-like and photocatalytic processes). Therefore, $FeNi_3/SiO_2/CuS/UV/H_2O_2$ can be used as a well-benefit treatment method for emerging non-biodegradable pollutants from aqueous solutions. The findings demonstrated that the designed degradation system had the highest removal efficiency of MTZ at natural pH, which makes this process highly beneficial. In addition, the removal efficiency of MTZ saw a remarkable rise with elevating of catalyst concentration. In the obtained optimum conditions from simulated wastewater, the evaluation of COD removal by the aforementioned process was performed in the real wastewater. The ability of nanocomposite to eliminate MTZ showed that it could be reused at least six times with suitable efficiency.

Declarations

All authors have read, understood, and have complied as applicable with the statement on "Ethical responsibilities of Authors" as found in the Instructions for Authors and are aware that with minor exceptions, no changes can be made to authorship once the paper is submitted. In addition, the authors of this study declare no competing interests.

Data availability statement

The authors of this study confirm that the data supporting the findings of this study are available within the manuscript.

Authorship contribution statement

Negin Nasseh: Editing, Methodology, and Experiments. Abolfazl Karimi Pour and Moslem Azqandi: Data analysis and Methodology. Waleed M.S Kassim: Supervision. Behnam Barikbin and Tariq J Al-Musawi: Writing, Results and Discussion and Editing.

Conflict of interest

The authors declare that they have no known competing financial interests or personal relationships that could have appeared to influence the work reported in this manuscript.

Funding

No funding was obtained for this study.

Acknowledgments

This article is taken from the research plan approved by Birjand University of Medical Sciences with the ethical code IR.BUMS.REC.1401.212. The authors are grateful to the Research Vice-Chancellor of Birjand University and the Faculty of Al-Mustakbal University for supporting this research.

References

[1] Z. Kang, X. Jia, Y. Zhang, X. Kang, M. Ge, D. Liu, C. Wang, Z. He, A review on application of biochar in the removal of pharmaceutical pollutants through adsorption and persulfate-based AOPs, Sustainability, 14 (2022) 10128, doi: 10.3390/su141610128.
[2] R. Akbarzadeh, A. Asadi, P.O. Oviroh, T.-C. Jen, One-pot synthesized visible light-driven BiOCl/AgCl/$BiVO_4$ n-p heterojunction for photocatalytic degradation of pharmaceutical pollutants, Materials, 12 (2019) 2297, doi: 10.3390/ma12142297.
[3] W. Cheng, M. Yang, Y. Xie, B. Liang, Z. Fang, E.P. Tsang, Enhancement of mineralization of metronidazole by the

electro-Fenton process with a Ce/SnO_2–Sb coated titanium anode, Chem. Eng. J., 220 (2013) 214–220.
[4] L. Wang, D. Luo, J. Yang, C. Wang, Metal-organic frameworks-derived catalysts for contaminant degradation in persulfate-based advanced oxidation processes, J. Cleaner Prod., 375 (2022) 134118, doi: 10.1016/j.jclepro.2022.134118.
[5] B. Kakavandi, A. Takdastan, N. Jaafarzadeh, M. Azizi, A. Mirzaei, A. Azari, Application of Fe_3O_4@C catalyzing heterogeneous UV-Fenton system for tetracycline removal with a focus on optimization by a response surface method, J. Photochem. Photobiol., A, 314 (2016) 178–188.
[6] C. Wang, R. Huang, R. Sun, J. Yang, M. Sillanpää, A review on persulfates activation by functional biochar for organic contaminants removal: synthesis, characterizations, radical determination, and mechanism, J. Environ. Chem. Eng., 9 (2021) 106267, doi: 10.1016/j.jece.2021.106267.
[7] Q. Wang, S. Tian, P. Ning, Ferrocene-catalyzed heterogeneous Fenton-like degradation of methylene blue: influence of initial solution pH, Ind. Eng. Chem. Res., 53 (2014) 6334–6340.
[8] R. Wang, X. Liu, R. Wu, B. Yu, H. Li, X. Zhang, J. Xie, S.-T. Yang, Fe_3O_4/SiO_2/C nanocomposite as a high-performance Fenton-like catalyst in a neutral environment, RSC Adv., 6 (2016) 8594–8600.
[9] L. Wang, H. Jiang, H. Wang, P.L. Show, A. Ivanets, D. Luo, C. Wang, MXenes as heterogeneous Fenton-like catalysts for removal of organic pollutants: a review, J. Environ. Chem. Eng., 10 (2022) 108954, doi: 10.1016/j.jece.2022.108954.
[10] M. Cheng, C. Lai, Y. Liu, G. Zeng, D. Huang, C. Zhang, L. Qin, L. Hu, C. Zhou, W. Xiong, Metal-organic frameworks for highly efficient heterogeneous Fenton-like catalysis, Coord. Chem. Rev., 368 (2018) 80–92.
[11] X. Li, K. Cui, Z. Guo, T. Yang, Y. Cao, Y. Xiang, H. Chen, M. Xi, Heterogeneous Fenton-like degradation of tetracyclines using porous magnetic chitosan microspheres as an efficient catalyst compared with two preparation methods, Chem. Eng. J., 379 (2020) 122324, doi: 10.1016/j.cej.2019.122324.
[12] S. Xin, G. Liu, X. Ma, J. Gong, B. Ma, Q. Yan, Q. Chen, D. Ma, G. Zhang, M. Gao, Y. Xin, High efficiency heterogeneous Fenton-like catalyst biochar modified $CuFeO_2$ for the degradation of tetracycline: economical synthesis, catalytic performance and mechanism, Appl. Catal., B, 280 (2021) 119386, doi: 10.1016/j.apcatb.2020.119386.
[13] X. Liu, Q. Zhang, B. Yu, R. Wu, J. Mai, R. Wang, L. Chen, S.-T. Yang, Preparation of Fe_3O_4/TiO_2/C nanocomposites and their application in Fenton-like catalysis for dye decoloration, Catalysts, 6 (2016) 146, doi: 10.3390/catal6090146.
[14] H. Wang, T. Chen, D. Chen, X. Zou, M. Li, F. Huang, F. Sun, C. Wang, D. Shu, H. Liu, Sulfurized oolitic hematite as a heterogeneous Fenton-like catalyst for tetracycline antibiotic degradation, Appl. Catal., B, 260 (2020) 118203, doi: 10.1016/j.apcatb.2019.118203.
[15] R. Yang, Q. Peng, B. Yu, Y. Shen, H. Cong, Yolk-shell Fe_3O_4@MOF-5 nanocomposites as a heterogeneous Fenton-like catalyst for organic dye removal, Sep. Purif. Technol., 267 (2021) 118620, doi: 10.1016/j.seppur.2021.118620.
[16] Z. Yang, P. Zhu, C. Yan, D. Wang, D. Fang, L. Zhou, Biosynthesized schwertmannite@biochar composite as a heterogeneous Fenton-like catalyst for the degradation of sulfanilamide antibiotics, Chemosphere, 266 (2021) 129175, doi: 10.1016/j.chemosphere.2020.129175.
[17] Y. Zhao, J.J. Tang, A. Motavalizadehkakhky, S. Kakooei, S.M. Sadeghzadeh, Synthesis and characterization of a novel CNT-$FeNi_3$/DFNS/Cu(II) magnetic nanocomposite for the photocatalytic degradation of tetracycline in wastewater, RSC Adv., 9 (2019) 35022–35032.
[18] N. Nasseh, L. Taghavi, B. Barikbin, M.A. Nasseri, Synthesis and characterizations of a novel $FeNi_3$/SiO_2/CuS magnetic nanocomposite for photocatalytic degradation of tetracycline in simulated wastewater, J. Cleaner Prod., 179 (2018) 42–54.
[19] S. Zarei, N. Farhadian, R. Akbarzadeh, M. Pirsaheb, A. Asadi, Z. Safaei, Fabrication of novel 2D Ag-TiO_2/γ-Al_2O_3/chitosan nano-composite photocatalyst toward enhanced photocatalytic reduction of nitrate, Int. J. Biol. Macromol., 145 (2020) 926–935.
[20] M. Arumugam, M.Y. Choi, Recent progress on bismuth oxyiodide (BiOI) photocatalyst for environmental remediation, J. Ind. Eng. Chem., 81 (2020) 237–268.
[21] A. Asadi, N. Daglioglu, T. Hasani, N. Farhadian, Construction of Mg-doped ZnO/g-C_3N_4@ZIF-8 multi-component catalyst with superior catalytic performance for the degradation of illicit drug under visible light, Colloids Surf., A, 650 (2022) 129536, doi: 10.1016/j.colsurfa.2022.129536.
[22] O.D. Arefieva, M.S. Vasilyeva, L.A. Zemnukhova, A.S. Timochkina, Heterogeneous photo-Fenton oxidation of lignin of rice husk alkaline hydrolysates using Fe-impregnated silica catalysts, Environ. Technol., 42 (2021) 2220–2228.
[23] A. Alizadeh, M. Fakhari, Z. Safaei, M.M. Khodeai, E. Repo, A. Asadi, Ionic liquid-decorated Fe_3O_4@SiO_2 nanocomposite coated on talc sheets: an efficient adsorbent for methylene blue in aqueous solution, Inorg. Chem. Commun., 121 (2020) 108204, doi: 10.1016/j.inoche.2020.108204.
[24] W. Liu, J. Zhou, D. Liu, S. Liu, X. Liu, S. Xiao, Enhancing electronic transfer by magnetic iron materials and metal-organic framework via heterogeneous Fenton-like process and photocatalysis, Mater. Sci. Semicond. Process., 135 (2021) 106096, doi: 10.1016/j.mssp.2021.106096.
[25] M.A. Nasseri, S.M. Sadeghzadeh, A highly active $FeNi_3$–SiO_2 magnetic nanoparticles catalyst for the preparation of 4H-benzo[b]pyrans and spirooxindoles under mild conditions, J. Iran. Chem. Soc., 10 (2013) 1047–1056.
[26] M.H. Beyki, M. Shirkhodaie, F. Shemirani, Polyol route synthesis of a Fe_3O_4@CuS nanohybrid for fast preconcentration of gold ions, Anal. Methods, 8 (2016) 1351–1358.
[27] D.H. Carrales-Alvarado, R. Ocampo-Pérez, R. Leyva-Ramos, J. Rivera-Utrilla, Removal of the antibiotic metronidazole by adsorption on various carbon materials from aqueous phase, J. Colloid Interface Sci., 436 (2014) 276–285.
[28] J. Bolobajev, M. Trapido, N. Dulova, Application of different techniques for activation of H_2O_2/Fe^{3+} system: a comparative study, J. Adv. Oxid. Technol., 18 (2015) 347–352.
[29] P.M. Martins, H. Salazar, L. Aoudjit, R. Gonçalves, D. Zioui, A. Fidalgo-Marijuan, C.M. Costa, S. Ferdov, S. Lanceros-Mendez, Crystal morphology control of synthetic giniite for enhanced photo-Fenton activity against the emerging pollutant metronidazole, Chemosphere, 262 (2021) 128300, doi: 10.1016/j.chemosphere.2020.128300.
[30] A. Eslami, M.M. Amini, A.R. Yazdanbakhsh, A. Mohseni-Bandpei, A.A. Safari, A. Asadi, N,S co-doped TiO_2 nanoparticles and nanosheets in simulated solar light for photocatalytic degradation of non-steroidal anti-inflammatory drugs in water: a comparative study, J. Chem. Technol. Biotechnol., 91 (2016) 2693–2704.
[31] F. Deng, F. Zhong, D. Lin, L. Zhao, Y. Liu, J. Huang, X. Luo, S. Luo, D.D. Dionysiou, One-step hydrothermal fabrication of visible-light-responsive $AgInS_2$/$SnIn_4S_8$ heterojunction for highly-efficient photocatalytic treatment of organic pollutants and real pharmaceutical industry wastewater, Appl. Catal., B, 219 (2017) 163–172.
[32] S. Pan, T. Zhao, H. Liu, X. Li, M. Zhao, D. Yuan, T. Jiao, Q. Zhang, S. Tang, Enhancing ferric ion/sodium percarbonate Fenton-like reaction with tungsten disulfide cocatalyst for metronidazole decomposition over wide pH range, Chem. Eng. J., 452 (2023) 139245, doi: 10.1016/j.cej.2022.139245.
[33] S. Talwar, A.K. Verma, V.K. Sangal, Modeling and optimization of fixed mode dual effect (photocatalysis and photo-Fenton) assisted metronidazole degradation using ANN coupled with genetic algorithm, J. Environ. Manage., 250 (2019) 109428, doi: 10.1016/j.jenvman.2019.109428.
[34] Y. Zhang, J. Zhou, X. Chen, L. Wang, W. Cai, Coupling of heterogeneous advanced oxidation processes and photocatalysis in efficient degradation of tetracycline hydrochloride by Fe-based MOFs: synergistic effect and degradation pathway, Chem. Eng. J., 369 (2019) 745–757.
[35] G. Fan, X. Zheng, J. Luo, H. Peng, H. Lin, M. Bao, L. Hong, J. Zhou, Rapid synthesis of Ag/AgCl@ZIF-8 as a highly efficient photocatalyst for degradation of acetaminophen under visible light, Chem. Eng. J., 351 (2018) 782–790.

[36] M. Farzadkia, A. Esrafili, M.A. Baghapour, Y.D. Shahamat, N. Okhovat, Degradation of metronidazole in aqueous solution by nano-ZnO/UV photocatalytic process, Desal. Water Treat., 52 (2014) 4947–4952.
[37] S. Ni, Z. Fu, L. Li, M. Ma, Y. Liu, Step-scheme heterojunction g-C_3N_4/TiO_2 for efficient photocatalytic degradation of tetracycline hydrochloride under UV light, Colloids Surf., A, 649 (2022) 129475, doi: 10.1016/j.colsurfa.2022.129475.
[38] G.H. Safari, M. Hoseini, M. Seyedsalehi, H. Kamani, J. Jaafari, A.H. Mahvi, Photocatalytic degradation of tetracycline using nanosized titanium dioxide in aqueous solution, Int. J. Environ. Sci. Technol., 12 (2015) 603–616.
[39] S. Azimi, A. Nezamzadeh-Ejhieh, Enhanced activity of clinoptilolite-supported hybridized PbS–CdS semiconductors for the photocatalytic degradation of a mixture of tetracycline and cephalexin aqueous solution, J. Mol. Catal. A: Chem., 408 (2015) 152–160.
[40] Y. Zhou, S. Feng, X. Duan, W. Wu, Z. Ye, X. Dai, Y. Wang, X. Cao, Stable self-assembly Cu_2O/ZIF-8 heterojunction as efficient visible light responsive photocatalyst for tetracycline degradation and mechanism insight, J. Solid State Chem., 305 (2022) 122628, doi: 10.1016/j.jssc.2021.122628.
[41] Y. Kuang, Q. Wang, Z. Chen, M. Megharaj, R. Naidu, Heterogeneous Fenton-like oxidation of monochlorobenzene using green synthesis of iron nanoparticles, J. Colloid Interface Sci., 410 (2013) 67–73.
[42] K.M. Reza, A. Kurny, F. Gulshan, Photocatalytic degradation of methylene blue by magnetite+H_2O_2+UV process, Int. J. Environ. Sci. Dev., 7 (2016) 325–329.
[43] D. Hamad, M. Mehrvar, R. Dhib, Experimental study of polyvinyl alcohol degradation in aqueous solution by UV/H_2O_2 process, Polym. Degrad. Stab., 103 (2014) 75–82.
[44] H.B. Ammar, M.B. Brahim, R. Abdelhédi, Y. Samet, Enhanced degradation of metronidazole by sunlight via photo-Fenton process under gradual addition of hydrogen peroxide, J. Mol. Catal. A: Chem., 420 (2016) 222–227.
[45] H. Cai, T. Zhao, Z. Ma, J. Liu, Efficient removal of metronidazole by the photo-Fenton process with a magnetic Fe_3O_4@PBC composite, J. Environ. Eng., 146 (2020) 04020056, doi: 10.1061/(ASCE)EE.1943-7870.000173.
[46] M. Farzadkia, E. Bazrafshan, A. Esrafili, J.-K. Yang, M. Shirzad-Siboni, Photocatalytic degradation of metronidazole with illuminated TiO_2 nanoparticles, J. Environ. Health Sci. Eng., 13 (2015) 35, doi: 10.1186/s40201-015-0194-y.
[47] A. Seidmohammadi, Y. Vaziri, A. Dargahi, H.Z. Nasab, Improved degradation of metronidazole in a heterogeneous photo-Fenton oxidation system with PAC/Fe_3O_4 magnetic catalyst: biodegradability, catalyst specifications, process optimization, and degradation pathway, Biomass Convers. Biorefin., 13 (2023) 9057–9073.